PIBB 生物化学与生物物理进展
Progress in Biochemistry and Biophysics
2018, 45(10): 1054~1067
www.pibb.ac.cn

Interaction of The Checkpoint Protein Rad9 and The Non-homologous End-joining Protein Ku70*

FAN Ying-Jun[1,2)**], LIU Yu-Heng[1,2)**], WANG Yu-Lan[1,2)**], KONG Bing-Jie[1,2)],
ZHAO Yun[1)], YE Chen[1)], AN Li-Li[1)***], HANG Hai-Ying[1)***]
([1)] *Key Laboratory for Protein and Peptide Pharmaceuticals, National Laboratory of Biomacromolecules, Institute of Biophysics, Chinese Academy of Sciences, Beijing* 100101, China;
[2)] *University of Chinese Academy of Sciences, Beijing* 100049, China)

Abstract Rad9 plays roles in both cell cycle checkpoint control and DNA repair. It can interact with the components of multiple DNA repair pathways and regulate their functions. Non-homologous end-joining (NHEJ) repair pathway is predominantly used in vertebrates for the repair of DNA double strand break (DSB). Proper activation of DNA-dependent protein kinase (DNA-PK), composed of Ku70, Ku80, and DNA-dependent protein kinase catalytic subunit (DNA-PKcs), is essential for NHEJ repair. In this study, we found that Rad9 interacts with Ku70 physically and functionally. Deletion of *Rad9* gene, knockdown of Rad9 expression or removal of Rad9 protein led to inefficient DNA end-joining repair. Furthermore, loss of Rad9 impaired the DNA damage-induced binding of Ku70 to the chromatin and attenuated the DNA damage-induced kinase activity of DNA-PKcs. Taken together, our data unveil a novel functional interplay between Rad9 and the NHEJ protein Ku70, indicating a role of Rad9 in NHEJ repair through modulating the activation of the DNA-PKcs/Ku70/Ku80 complex.

Key words Rad9, NHEJ, Ku70, DNA-PKcs
DOI: 10.16476/j.pibb.2018.0163

DNA repair and cell cycle checkpoint cooperate in protecting cells from intracellular and environmental genotoxic stresses and maintaining genomic integrity [1]. The checkpoint protein Rad9 is evolutionarily conserved from yeast to humans and can form a ring-shaped heterotrimer with Hus1 and Rad1, dubbed Rad9-Hus1-Rad1 complex (9-1-1 complex)[2–5]. Rad9 is required for G2/M and S/M checkpoint activation [6–7]. In response to DNA damage, 9-1-1 complex is loaded onto DNA by Rad17 [8] and facilitates ATR activation and downstream phosphorylation, activating CHK1 kinase to arrest the cell cycle [9]. Aside from cell cycle checkpoint functions, there is mounting evidence that Rad9 plays important roles in multiple DNA repair pathways such as base excision repair, nucleotide excision repair and mismatch repair[10–19]. Currently, the generally accepted working model is that the 9-1-1 complex acts as a platform to recruit other proteins involved in cell cycle checkpoints and DNA repair[18, 20–22].

DNA double strand break (DSB) is one of the most toxic forms of DNA damage. Perturbations of DSB repair can lead to massive loss of genetic information and are often associated with premature aging, tumorigenesis and cell death. There are two principal DSB repair pathways: homologous recombination (HR) [23] and non-homologous end-joining (NHEJ) repair[24]. HR is largely error free,

* This work was supported by grants from The National Natural Science Foundation of China (31370792, U1738112).
**These authors contributed equally to this work.
***Corresponding author.
AN Li-Li. Tel: +86-10-64888268, E-mail: afxdxz@163.com
HANG Hai-Ying. Tel: +86-10-64888473, E-mail: hh91@ibp.ac.cn
Received: June 11, 2018 Accepted: August 29, 2018

requiring a homologous sequence to guide repair. Thus it is more prevalent after DNA replication. NHEJ promotes direct ligation of the DSB ends in an error-prone manner. It is active throughout the cell cycle and is favored in G1 cells [25]. NHEJ is predominantly used in vertebrates for the repair of DSB[24]. Key factors involved in NHEJ pathway include the Ku70/80 heterodimer, the DNA-dependent protein kinase catalytic subunit (DNA-PKcs), Artemis, X-ray repair complementing defective repair in Chinese hamster cells 4 (XRCC4), DNA ligase Ⅳ, and XRCC4-like factor (XLF) [26]. The Ku70/80 (Ku) heterodimer is a structure-specific, sequence-independent DNA binding protein complex with a strong binding constant (～10^{-9} mol/L) between Ku70 and Ku80[27–28]. Structural studies of the Ku heterodimer reveal that it exists as a preformed asymmetric ring structure that encircles duplex DNA [29]. After binding to DSB ends, the regulatory subunit Ku heterodimer can recruit the catalytic subunit DNA-PKcs and trigger its serine/threonine kinase activity forming an active DNA-dependent protein kinase (DNA-PK) [30]. DNA-PK is central in NHEJ. It initially recognizes and binds damaged DNA, recruits other repair factors as a scaffold and alters the activity of other DNA repair factors *via* serine/threonine phosphorylation[31–33]. Growing evidence suggests that 9-1-1 complex plays important roles in DSB repair. The deletion of each of the three genes made cells highly sensitive to ionizing radiation in organisms from yeast to humans [6, 34–39]. After ionizing radiation, Rad9 rapidly accumulates into nuclear foci [20] and becomes more firmly anchored to chromatin [21]. Rad9 can also rapidly bind DNA containing DSB and is required for the damage-dependent focus formation of topoisomerase Ⅱβ binding protein 1 (a checkpoint protein)[22]. It has been demonstrated that components of 9-1-1 complex play an important role in HR[38–40]. Furthermore, Tsai *et al* [41] reported that knockdown of Rad9 significantly reduced the HR frequency and increased the alternative NHEJ frequency. In this study, we reported for the first time that Rad9 can interact with Ku70 physically and functionally. In Rad9-knockout mouse embryonic stem cells, Ku70 was deficient in the DNA damage-induced binding to chromatin and DNA-PK activation was impaired. We also provided evidence that dysfunction of Rad9 impaired the NHEJ efficiency. Collectively, our study implied a novel role of Rad9 in mediating the NHEJ process *via* modulating the molecular activities of the DNA-PKcs/Ku70/Ku80 complex.

1 Materials and methods

1.1 Antibodies

Anti-Rad9 monoclonal antibody was purchased from BD Biosciences Pharmingen. anti-FLAG M2 monoclonal antibody (F1804), anti-FLAG polyclonal antibody (F7425), anti-His monoclonal antibody, anti-GST monoclonal antibody and anti-GAPDH monoclonal antibody were purchased from Sigma－Aldrich. Anti-Ku70 polyclonal antibody and anti-HA monoclonal antibody were purchased from Santa Cruz Biotechnology. Anti-Ku70 monoclonal antibody (N3H10) was purchased from Thermo. Anti-H3 monoclonal antibody was purchased from Cell Signaling Technology and anti-γH2AX monoclonal antibody was purchased from Upstate Technology. HRP-conjugated anti-mouse IgG (W4021) and HRP-conjugated anti-rabbit IgG (W4011) were purchased from Promega.

1.2 Cell lines, cell culture and DNA damaging agents

Human embryonic kidney (HEK) 293T cells and human HeLa cells were cultured in DMEM (Invitrogen) supplemented with 10% fetal bovine serum (Hyclone) and 10^5 U/L penicillin/streptomycin (Gibco). *mRad9*$^{+/+}$ mouse embryonic stem (mES) cells, *mRad9*$^{-/-}$ mES cells and *mRad9*$^{-/-}$ mES cells with ectopically expressing of mRad9 (*mRad9*$^{-/-}$+mRad9 mES cells), were obtained from Howard B. Lieberman's laboratory and were cultured as described previously[6, 17]. Briefly, cells were cultured in high glucose DMEM (Hyclone) supplemented with 15% fetal bovine serum (Hyclone), 2 mmol/L L-glutamine (Gibco), 100 μmol/L nonessential amino acids (Gibco), 100 μmol/L beta-mercaptoethanol (Amresco), 10^6 units/L leukemia inhibitory factor (LIF, Millipore), 10^5 U/L penicillin/streptomycin (Gibco). *mRad9*$^{-/-}$ mES cells were transfected with pZeoSV2-mRad9 and then challenged with 100 g/L zeocin to generate stable mutant cells ectopically expressing mRad9. The selected *mRad9*$^{-/-}$+mRad9 mES cells were cultured in the medium containing 25 g/L zeocin to maintain the transfected genes in the cells[6].

For DNA damaging treatments, cells were exposed to 100 μmol/L etoposide (Sigma) for 30 min.

1.3 Immunoprecipitation

Plasmids capable of expressing in human cells were constructed using the pCDNA3-6HA vector and the pFLAG-CMV2 vector (Sigma, St Louis, MO). To make pFLAG-CMV2-hKu70, the cDNA of the hKu70 gene was amplified by PCR. The pCDNA3-6HA construct bearing the hHus1, hRad1 or hRad9 open reading frame were constructed previously[42].

Transfections were conducted in HEK 293T cells with Lipofectamine and Plus reagent (Invitrogen). Cells were seeded 24 h prior to transfection to achieve 60%～80% confluence in 60 mm tissue culture dishes and co-transfected with 1.5 μg pFLAG-CMV2 DNA and 1.5 μg pCDNA3-6HA DNA following the protocol described by Invitrogen. Cells were collected 20 h after transfection and lysed in lysis buffer [150 mmol/L NaCl, 50 mmol/L Tris-HCl, pH 7.5, 10% glycerol, 0.5% NP-40, 1× protease inhibitor cocktail (Roche)]. Co-immunoprecipitation and western blotting were performed as described previously[17].

Co-immunoprecipitation of endogenous Rad9 and Ku70 was performed using human HeLa cells and mES cells. Antibody coupled-Protein A beads were prepared by incubating 1 μg of Ku70 monoclonal antibody or mouse IgG with 50 μl Protein A resin (Invitrogen) overnight at 4℃. Cells were lysed as mentioned above and pre-cleared by mouse IgG (Santa Cruz Biotechnology). Then the pre-cleared cell lysis and the antibody coupled-Protein A beads were incubated for 4 h at 4℃. SDS-PAGE and western blot were performed accordingly.

1.4 In vitro pull-down assays

Plasmids capable of expressing in *E. coli* cells were constructed using the pGEX-6P-1 vector (GE Health) and the pET24a (+) vector (Novagen). The plasmids of pGEX-6P-1-hRad9/hRad1/hHus1 and pET24a (+)-hRad9 were generated previously [17]. To make pGEX-6P-1-hKu70 and pET24a (+)-hKu70 constructs, the Ku70 gene was amplified by PCR from pFLAG-CMV2-hKu70.

Expression of GST-tagged proteins and His-tagged proteins were performed in Rosetta cells (Invitrogen). Purification of GST-tagged proteins and His-tagged proteins were conducted using the 50% slurry of glutathione-Sepharose 4B (GE Healthcare) and the 50% slurry of Ni Sepharose High Performance (Amersham Biosciences) as previously described[17].

100 ng His-tagged proteins were added to the appropriate GST-tagged protein-coupled glutathione-Sepharose 4B and incubated for 1 h in 500 μl binding buffer (50 mmol/L Tris-HCl, pH 7.5, 150 mmol/L NaCl, 10 mmol/L $MgCl_2$, 10% glycerol, 1% TritonX-100, 0.5 mmol/L DTT, 1% BSA) at 4℃. After centrifugation at 500 g for 5 min, the pellets were washed for 5 times with 500 μl of binding buffer at 4℃ and fractionated on a 10% SDS-PAGE gel. A control of immobilized GST alone was run concurrently.

1.5 siRNA transfection

Small interference RNA(siRNA) duplexes against human Rad9 (5′ AAGUCUUUCCUGUCUGUCUUC 3′)[19] were synthesized by Invitogen Inc. Transfection experiments were carried out using Lipofectamin RNAiMAX Reagent (Invitrogen) following the manufacture's instructions.

1.6 Plasmid based in vitro end-joining assay

Plasmid based *in vitro* end-joining assay was performed according to Iliakis, G. *et al*[43] with minor modifications. Whole-cell extracts (WCE) of mES cells and HEK 293T cells were extracted by the Nuclear Extract Kit from Active Motif. Protein concentration was determined by the Bradford assay. The plasmid pBlueScript was used in this assay. Supercoiled plasmid DNA was prepared by using two-step purification on CsCl-ethidium bromide gradient. It was used as a substrate in DNA end-joining reactions following digestion with *Eco*R Ⅰ (Takara) to generate linearized DNA. End-joining reactions were performed in 20 mmol/L HEPES-KOH (pH 7.5), 10 mmol/L $MgCl_2$, 80 mmol/L KCl, 1 mmol/L ATP, 1 mmol/L DTT, 100 ng of DNA and 0–1 μg WCE from mES or HEK 293T cells in a final volume of 20 μl at 25℃ for 1 h. Reactions were terminated by adding 2 μl of 0.5% SDS, 2 μl of 0.5 mol/L EDTA and 1 μl of Proteinase K (10 g/L), then incubated for 1 h at 37℃. One half of the reaction was loaded on a 0.7% agarose gel and run at 45 V (2 V/cm) for 5 h. Gels were stained in ethidium bromide and scanned in an AlphaImager 2200 (Alpha Innotech). For quantification of the percentage of end-joining, the ImageQuant software (Molecular Dynamics) was used to calculate the fraction of input plasmid found in

rejoined products (dimers and multimer plasmids).

For antibody inhibition, anti-hRad9 antibody (0.5, 1 and 2 μg) or mouse IgG (0.5, 1 and 2 μg) were added to the end-joining reaction prior to the addition of ATP and plasmid DNA. After incubation at 25℃ for 10 min, ATP and plasmid DNA were added to start the rejoining reaction.

1.7 Chromatin binding assay

The fractionation procedure followed the protocol published by Mendez J. and Stillman B[44] with some modifications. Typically, 10^7 mES cells, either treated with 100 μmol/L etoposide (Sigma) for 30 min or untreated, were harvested and rinsed twice with ice-cold phosphate-buffered saline. The cell pellet was re-suspended in buffer A [10 mmol/L HEPES, pH 7.9, 10 mmol/L KCl, 1.5 mmol/L $MgCl_2$, 0.34 mol/L sucrose, 10% glycerol, 1 mmol/L DTT, 1× protease inhibitor cocktail (Roche), 0.1 mmol/L phenylmethyl-sulfonyl fluoride, 0.1% Triton X-100] and was incubated for 5 min on ice. Nuclei were collected in pellet by low-speed centrifugation (4 min, 1 300 *g*, 4℃), washed once in buffer A, and then lysed in buffer B (3 mmol/L EDTA, 0.2 mmol/L EGTA, 1 mmol/L DTT, protease inhibitors as described above) for 30 min on ice. Insoluble chromatin was collected by centrifugation (4 min, 1 700 *g*, 4℃), washed once in buffer B, and centrifuged again under the same conditions. To release chromatin-bound proteins by nuclease treatment, insoluble chromatin was re-suspended in micrococcal nuclease buffer and incubated at 37℃ for 15 min with 0.2 U of micrococcal nuclease (Fermantas). The nuclease reaction was stopped by the addition of 1 mmol/L EGTA. The final chromatin pellet was collected by low-speed centrifugation and re-suspended in Laemmli buffer. SDS-PAGE and Western blot were performed accordingly.

1.8 DNA-PK kinase activity assay

DNA-PK kinase activity was measured with the SignaTECT™ DNA-Dependent Protein kinase assay system (Promega) following manufacturer's instructions. Briefly, a biotinylated DNA-PK p53-derived substrate and γ-^{32}P labeled ATP was incubated in reaction buffer at 30℃ for 5 min. Then the cell nuclear extract was added and the reaction was incubated for another 5 min. The kinase reaction was terminated with the termination buffer. The ^{32}P-labeled DNA-PK biotinylated peptide substrate specifically bound to the biotin capture membrane. The unbound components of the reaction were removed *via* extensive washing. The amount of ^{32}P incorporated into the DNA-PK biotinylated peptide substrate was determined by liquid scintillation counter (Perkin Elmer).

1.9 Statistical analysis

The results are presented as mean ± SEM. Statistical significance was determined by Student's *t*-test. *P*-values of less than 0.05 were considered statistically significant.

2 Results

2.1 Rad9 associates with Ku70 in cells

Growing evidence suggests that 9-1-1 complex plays important roles in DSB repair[6, 20–22, 34–40]. We have identified many Rad9-associated proteins which are not previously reported to interact with hRad9 using a strategy of immunoaffinity-Mass spectrometry [17]. Interestingly, one of these proteins was Ku70, a critical protein in NHEJ repair. Previously, none of the proteins directly involved in NHEJ has been reported to associate with Rad9. Therefore, we characterized this interaction and its functional significance further.

To confirm the association of Ku70 and Rad9, co-immunoprecipitation was performed after co-transfection of pFLAG-CMV2-hKu70 and pCDNA3-6HA-hRad9. The results showed that HA-tagged hRad9 (HA-hRad9) interacted with Flag-tagged hKu70 (Flag-hKu70) in HEK 293T cells, and did not interact with the negative control Flag-GFP (Figure 1a). Importantly, endogenous Rad9 and Ku70 were immunoprecipitated together from both the extracts of HeLa cells and the extracts of mES cells by Ku70 monoclonal antibody, but not by the negative control (IgG, Figure 1b). These data indicate that Rad9 associates together with Ku70 in cells.

2.2 Direct interaction of the N-terminal region of hRad9 with hKu70

Then, we determined whether the interaction between Rad9 and Ku70 was direct. We performed *in vitro* GST pull-down assay using recombinant hRad9 and hKu70 proteins. GST-hKu70 fusion protein bound to glutathione-Sepharose was incubated with purified His-hRad9 protein. hMLH1 was reported to interact with hRad9 directly [17] and was used as a positive control in this study. His-hRad9 was pulled down by GST-hKu70 as well as GST-hMLH1, but could not be

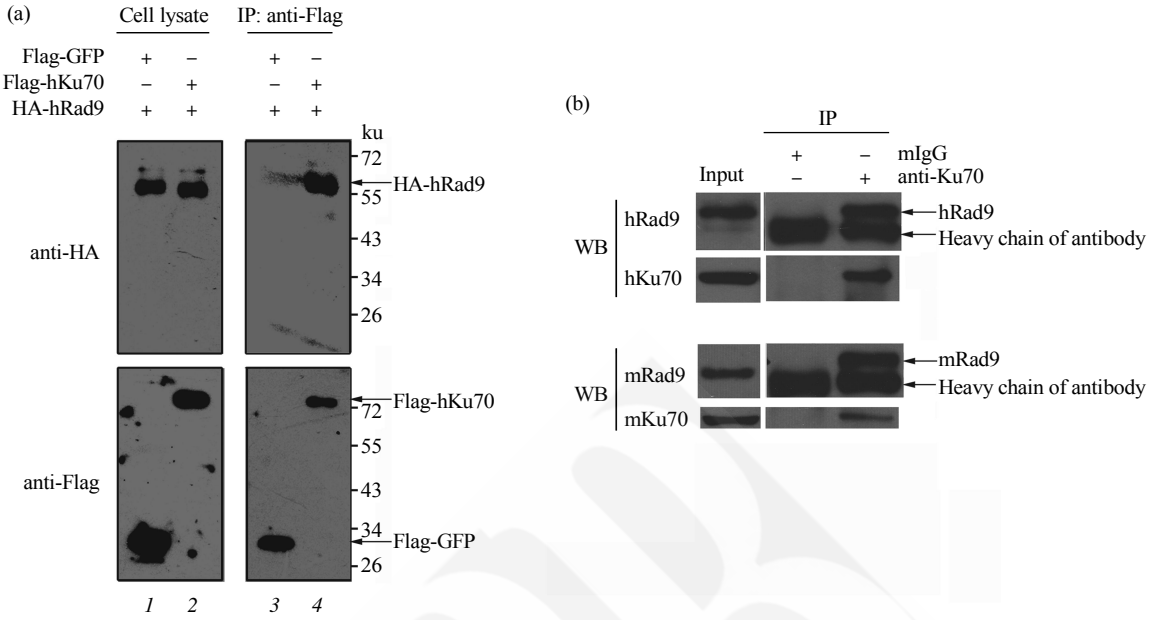

Fig. 1 Rad9 associated with Ku70

(a) Co-immunoprecipitation of Flag-hKu70 and HA-hRad9 was performed. pCDNA3-6HA-hRad9 was transfected into HEK 293T cells along with pFLAG-CMV2-hKu70 (lanes *2* and *4*) and pFLAG-CMV2-GFP (lanes *1* and *3*: negative control). The lysates were immunoprecipitated with anti-FLAG antibody, and blotting membrane was probed with antibodies against HA (upper) and against Flag (lower). (b) Co-immunoprecipitation of endogenous Rad9 and Ku70 in human HeLa cells (the upper panel) and in mES cells (the lower panel) was performed. Endogenous Rad9 was immunoprecipitated with anti-Ku70 monoclonal antibodies (lane *2*), but not with mouse IgG (lane *3*). The immunoprecipitated proteins were detected with antibodies against Rad9 (upper) and Ku70 (lower). Ten percent of the lysate was used for the loading control and the remaining 90% for co-immunoprecipitation. mIgG, mouse IgG; IP, immunoprecipitation; WB, Western blot.

precipitated by GST alone(Figure 2a). Furthermore, we reversed the GST and His tag to exclude the potential unexpected effect of these tags to the physical interaction. GST-hRad9 fusion protein bound to glutathione-Sepharose was incubated with purified His-hKu70 protein. His-hKu70 was pulled down by GST-hRad9, while GST alone could not bind to His-hKu70 (Figure 2b). These results confirmed that Rad9 and Ku70 interacted physically.

To investigate which region of the hRad9 protein was responsible for mediating the interaction with hKu70, full length hRad9 was split into fragments and tested for their abilities to interact with full-length hKu70 in a GST pull-down assay. GST-tagged fragments of hRad9 were immobilized on glutathione-Sepharose and incubated with His-hKu70, and as a negative control, GST alone with His-hKu70 was included. Our results showed that the hKu70-interacting region of hRad9 was localized to residues 35aa-54aa (Figure 2c and 2d).

2.3 No direct interaction between Ku70 and 9-1-1 components Rad1 and Hus1

It has been shown that Rad9, Rad1 and Hus1 form a heterotrimeric complex[3–5, 45]. We asked whether Rad1 and Hus1 could also physically interact with Ku70, as Rad9 did. As revealed by co-immunoprecipitation assay (Figure 3a), HA-Rad1 and HA-Hus1 co-immunoprecipitated with Flag-hKu70. However, compared to HA-hRad9, the co-immunoprecipitation between HA-hRad1/ HA-hHus1 and Flag-hKu70 was very weak. These results suggest that Ku70 weakly binds to Rad1 and Hus1 *in vivo* probably through Rad9.

To confirm whether Rad1 and Hus1 interact with Ku70 physically, we performed GST-pull down assay mentioned above. GST-hRad9, GST-hRad1 and GST-hHus1 fusion protein bound to glutathione-Sepharose were incubated with purified His-hKu70 protein. His-hKu70 was pulled down by GST-hRad9, while GST-hRad1 and GST-hHus1 failed to pull down His-hKu70 (Figure 3b). These results indicate that Rad1 and Hus1 do not interact with Ku70 directly. The weak interaction of Rad1 and Hus1 with Ku70 observed in co-immunoprecipitation assay was probably mediated by Rad9.

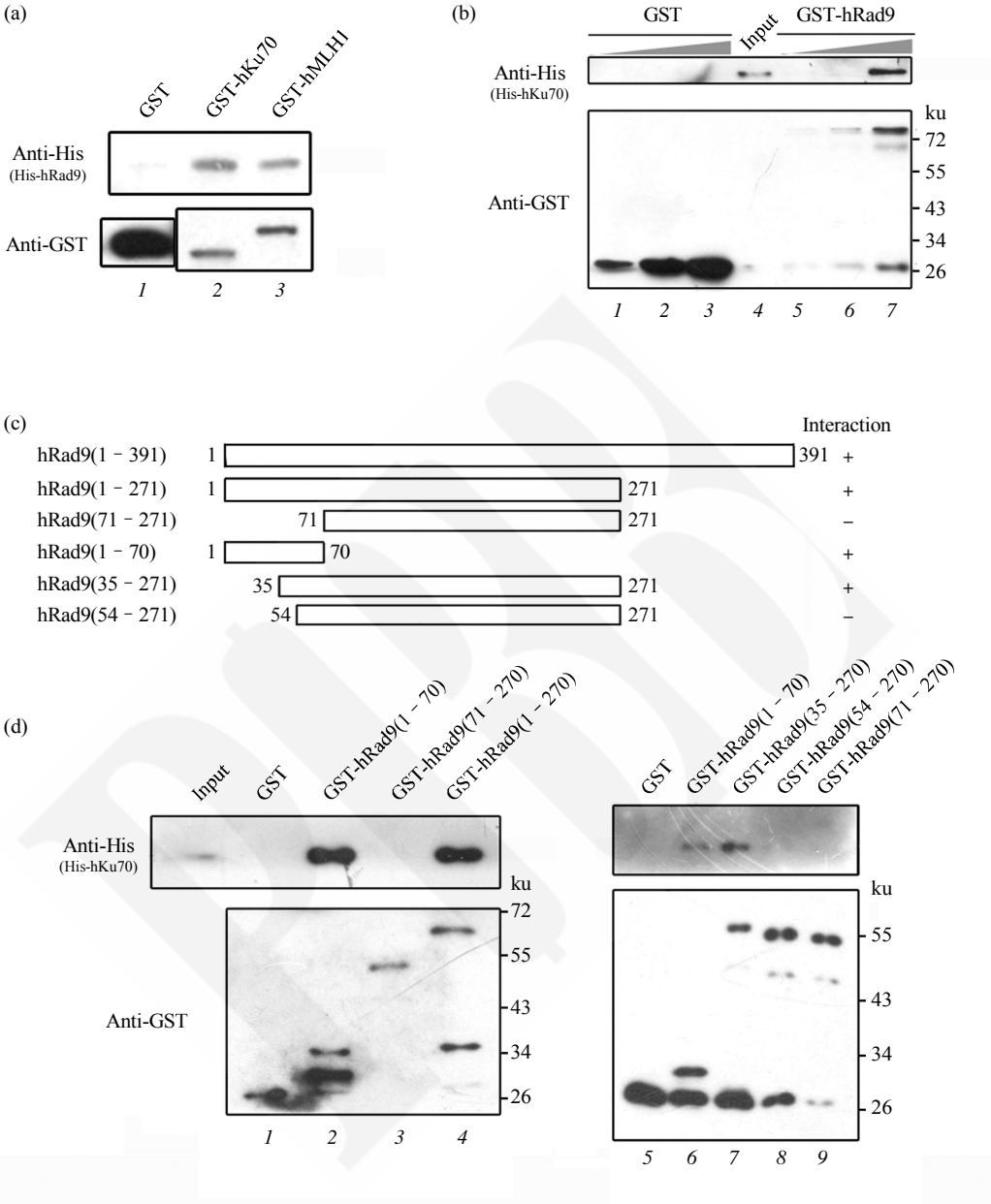

Fig. 2　Direct interaction of the N-terminal region of hRad9 with hKu70

GST pull-down assay was performed. (a) One microgram GST alone (lane *1*, negative control), one microgram GST-hKu70 (lane *2*) or one microgram GST-hMLH1 (lane *3*, positive control) was immobilized on glutathione-Sepharose and incubated with purified His-hRad9 (100 ng) in binding buffer. The purified proteins were subjected to western blot analysis and probed with the anti-His antibody (the upper panel) or anti-GST monoclonal antibody (the lower panel). GST-hKu70 and GST-hMLH1 were able to pull down His-hRad9. (b) One microgram (lane *5*), two microgram (lane *6*) and three microgram (lane *7*) GST-hRad9 or corresponding the equal amount of GST alone (lane *1* – *3*) was immobilized on glutathione-Sepharose and incubated with purified His-hKu70 (100 ng). Lane *4* contains 10 ng (10% of the total input) of His-hKu70. GST-hRad9 was able to pull down His-hKu70 in a dose dependent manner. In lanes *5*, *6* and *7*, the strips at the bottom (26 ku) were degraded GST proteins from GST-hRad9. (c) The map schematically illustrates the regions of hRad9 that interact with hKu70. The results were derived from the experimental data in Figure 2d. The intact hRad9 contains 391 amino acid residues. '+' stands for positive and '-' for negative. (d) One microgram GST alone, one microgram GST-hRad9 (1-70), one microgram GST-hRad9 (71 –270), or one microgram GST-hRad9 (1 –270) was immobilized on glutathione-Sepharose and incubated with purified His-hKu70. The Ku70-interacting region of Rad9 is localized to residues 1-70aa (the left part). To further narrow down the Ku70-interacting region of Rad9, one microgram GST alone, one microgram GST-Rad9 (1–70), one microgram GST-Rad9 (35–270), one microgram GST-Rad9 (54–270) or one microgram GST-Rad9 (71 –270) was immobilized on glutathione-Sepharose and incubated with purified His-hKu70. The Ku70-interacting region of Rad9 was localized to residues 35 –54aa (the right part). In lanes *6* – *9*, the strips at the bottom (26 ku) were degraded GST proteins from the corresponding GST fusion proteins.

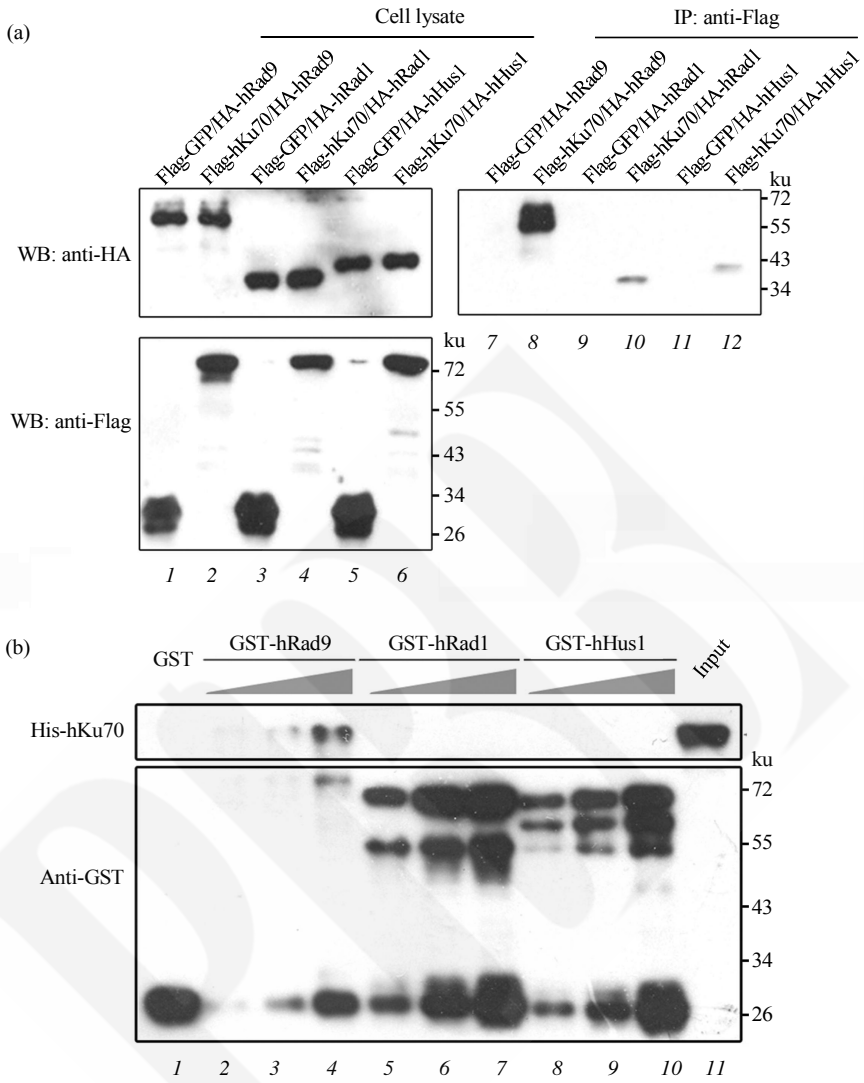

Fig. 3　Rad1 and Hus1 does not interacted with Ku70 physically

(a) Co-immunoprecipitation assay was performed. pFLAG-CMV2-hKu70 (lanes *2*, *4*, *6*, *8*, *10* and *12*) or pFLAG-CMV2-GFP (lanes *1*, *3*, *5*, *7*, *9* and *11*: negative control) was transfected into HEK 293T cells along with pCDNA3-6HA-hRad9 (lane *1*, *2*, *7* and *8*), pCDNA3-6HA-hRad1 (lane *3*, *4*, *9* and 10) or pCDNA3-6HA-hHus1 (lane *5*, *6*, *11* and *12*). Ten percent of the lysate was used for the loading control and the remaining 90% for co-immunoprecipitation. The lysate was immunoprecipitated with anti-FLAG antibody, and the Western blot membrane was probed with the antibody against HA (upper) and against FLAG (lower). (b) GST pull-down assay was performed. One microgram (lane *2*), two microgram (lane *3*) and three microgram (lane *4*) GST-hRad9, corresponding the equal amount of GST-Rad1 alone (lane *5*–*7*), corresponding the equal amount of GST-Hus1 (lane *8*–*10*) or three microgram GST alone (lane *1*) was immobilized on glutathione-Sepharose and incubated with purified His-hKu70 (100 ng). Lane *11* contained 10 ng (10% of the total input) of His-hKu70. In lanes *2*–*10*, the strips at the bottom (26 ku) were degraded GST proteins from the corresponding GST fusion proteins.

2.4　Lack of Rad9 reduces the efficiency of DNA NHEJ repair

Ku70 is one of the key factors involved in NHEJ pathway. We asked whether hRad9 also functioned in NHEJ. γ-H_2AX is a broadly used maker of DNA DSB[46]. Using the *mRad9*$^{+/+}$ mES cells (wild-type mouse ES cells), *mRad9*$^{-/-}$ mES cells (mRad9-deleted mouse ES cells) and *mRad9*$^{-/-}$ +*mRad9* mES cells (ectopic expression of mRad9 in *mRad9*$^{-/-}$ mES cells at a level comparable to that in *mRad9*$^{+/+}$ cells) as a model

system, we detected γ-H_2AX expression in these cells by western blot analysis. *mRad9*$^{-/-}$ mES cells showed increased levels of γ-H_2AX expression(Figure 4a). The depletion of Rad9 accumulated a significantly increased level of spontaneous DSB without exogenous agents, which was consistent with our previous findings[47–48].

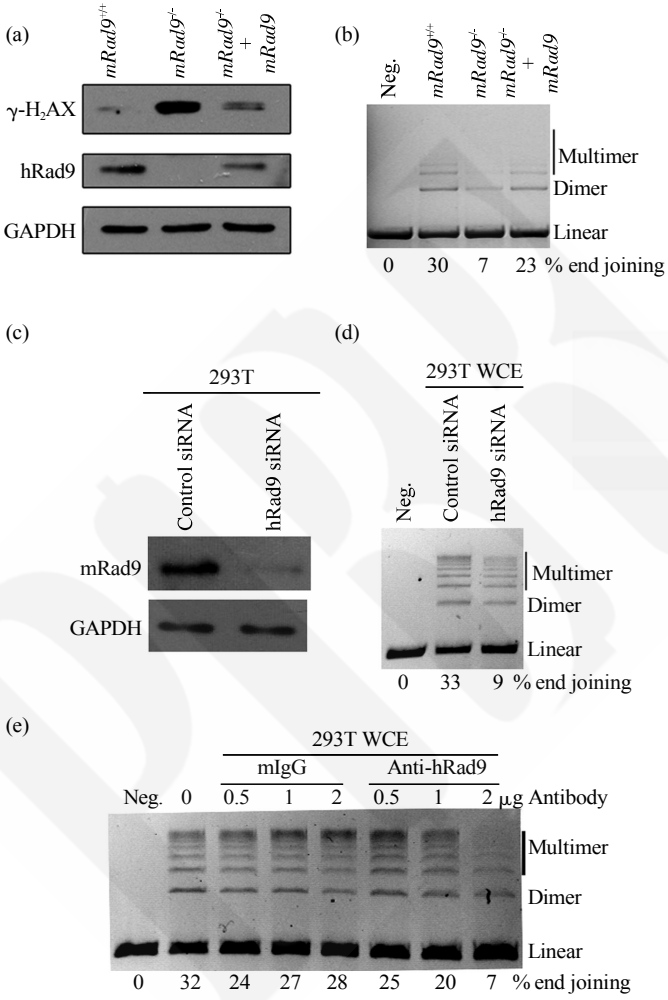

Fig. 4　Lack of Rad9 reduced the efficiency of DNA end-joining

(a) Western blot analysis was performed. Cell lysates from *mRad9*$^{+/+}$ mES cells, *mRad9*$^{-/-}$ mES cells and *mRad9*$^{-/-}$+*mRad9* mES cells were sequentially immunoblotted with antibody against γ-H_2AX (top, 17 ku), Rad9 (middle, 55 ku), and GAPDH (bottom, 36 ku). *mRad9*$^{-/-}$ mES cells showed increased levels of γ-H_2AX expression. (b) *In vitro* end-joining assay was performed. Plasmid pBlue Script DNA was linearized by digestion with *Eco*RⅠ. Reactions were assembled with the extracts from the *mRad9*$^{+/+}$ mES cells, *mRad9*$^{-/-}$ mES cells and *mRad9*$^{-/-}$+*mRad9* mES cells indicated on the top of each lane. After electrophoresis, the agarose gel was stained in ethidium bromide. The positions of the original linear plasmid and the rejoined products (dimmer and multimer plasmids) were indicated to the right of the gel. The percentage of end-joining shown at the bottom of each lane indicates the fraction of input plasmid found in rejoined products. *MRad9* deletion caused a 4 fold decrease in the end-joining efficiency and this decrease was compensated by reintroducing mRad9. *mRad9*$^{+/+}$ mES cells, wild-type mES cells; *mRad9*$^{-/-}$ mES cells, mRad9-deleted mES cells, *mRad9*$^{-/-}$+*mRad9* mES cells, ectopic expression of mRad9 in *mRad9*$^{-/-}$ mES cells. (c) Western blot analysis of the expression levels of hRad9 (55 ku) and GAPDH (36 ku) in HEK 293T cells transfected with control siRNA or hRad9 siRNA was performed. *HRad9* was knocked down in HEK 293T cells transiently expressing hRad9 siRNA. (d) *In vitro* end-joining assay was performed. Reactions were assembled with the extracts from HEK 293T cells transfected with control siRNA or hRad9 siRNA. HRad9 deletion in human cells also caused substantial decrease in the end-joining efficiency. (e) Antibody inhibition of hRad9 and *in vitro* end-joining assay were performed. Anti-hRad9 antibody (0.5 μg, 1 μg and 2 μg) or mouse IgG (0.5 μg, 1 μg and 2 μg) were added to the end-joining reaction. Reactions assembled with the Rad9-specific monoclonal antibody showed strong inhibition of the rejoining efficiency of dimers and multimers in a dose-dependent manner. mIgG, mouse IgG; WCE, whole-cell extracts.

Then we used *in vitro* non-homologous DNA end-joining assays to directly assess the role of Rad9 in DNA end-joining. WCE of *mRad9*$^{+/+}$ mES cells, *mRad9*$^{-/-}$ mES cells and *mRad9*$^{-/-}$+*mRad9* mES cells were incubated with linearized pBlueScript DNA substrate, which contained a DSB site generated by the endonuclease *Eco*RⅠ. *mRad9*$^{-/-}$ mES cells extracts had less efficient DNA end-joining compared to *mRad9*$^{+/+}$ mES cells extracts, and ectopically expressing *mRad9* in *mRad9*$^{-/-}$ mES cells compensated for the most of this defect(Figure 4b). Quantitatively, the end-joining efficiency of *mRad9*$^{-/-}$ mES cell extracts was around 7%, while the end-joining efficiency of *mRad9*$^{+/+}$ cell extracts was about 30%. After ectopically expressing of *mRad9*, the end-joining efficiency was elevated to 23%. Thus mRad9 deletion caused a 4 fold decrease in the end-joining efficiency and this decrease was partially compensated by reintroducing mRad9.

To test whether Rad9 plays the same role in human cells, we knocked down hRad9 expression in HEK 293T cells using siRNA. 48 h after transfection, the expression level of hRad9 in cells transfected with hRad9-specific siRNA dramatically reduced, compared to that in cells transfected with control siRNA (Figure 4c). DNA end-joining assay was performed accordingly with WCE of hRad9 or control siRNA treated cells. Similar to the results observed in mES cell extracts, the end-joining efficiency in extracts with hRad9 was 33% while the end-joining efficiency in extracts without hRad9 decreased to 9% (Figure 4d). Therefore, hRad9 knockdown in human cells also led to substantial decrease in the end-joining efficiency.

To further confirm this, we performed the antibody inhibition experiment in the extracts from HEK 293T cells. Compared to the reactions assembled with incremental concentrations of nonspecific mouse IgG, reactions assembled with the Rad9-specific monoclonal antibody showed strong inhibition of the rejoining efficiency of dimer and multimers in a dose-dependent manner (Figure 4e). In summary, these results provide evidence that Rad9 plays an important role in the NHEJ repair under the reaction conditions employed here.

2.5 Rad9 deletion impairs Ku70 binding to chromatin

The first step of NHEJ pathway is the binding of Ku70/80 heterodimer to DSB ends[24, 49]. Etoposide is a topoisomerase inhibitor known to induce double-stranded breaks in DNA [50]. We first checked the expression level of Ku70 in cell lysates of *mRad9*$^{+/+}$ mES cells, *mRad9*$^{-/-}$ mES cells and *mRad9*$^{-/-}$+*mRad9* mES cells with or without etoposide treatment (30 min). Neither loss of Rad9 nor DNA damage induced any obvious change of Ku70 expression (Figure 5a). This result was consistent with previous studies, which found that protein level of Ku rarely changes after DNA damage[29, 51]. Then we detected the expression of Ku70 in the chromatin-enriched fraction using the cell models mentioned above. After etoposide treatment, the level of Ku70 in the chromatin-enriched fraction increased to 2.83 times in *mRad9*$^{+/+}$ mES cells, 1.31 times in *mRad9*$^{-/-}$ mES cells and 2.79 times in *mRad9*$^{-/-}$+*mRad9* mES cells(Figure 5b). These results suggest that Ku70 recruitment is impaired in cells depleted of Rad9 after etoposide treatment.

2.6 Rad9 deletion causes attenuated DNA-PKcs kinase activity

DNA-PKcs is the catalytic subunit of DNA-PK and its kinase activity is crucial for the NHEJ repair process[31–33]. DNA-PKcs alone is inactive and relies on Ku proteins to recruit it to the broken DNA ends, which activates its kinase activity. As mentioned above, the binding of Ku70 to the DSB ends was compromised in Rad9-deleted cells. In order to check whether this compromise cause defective DNA-PKcs activation, we assayed DNA-PKcs kinase activity of the nuclear extracts from *mRad9*$^{+/+}$ mES cells, *mRad9*$^{-/-}$ mES cells and *mRad9*$^{-/-}$+*mRad9* mES cells with or without etoposide treatment (30 min) by detecting the amount of ^{32}P incorporated into the peptide substrate of DNA-PK using the SignaTECT™ DNA-Dependent Protein kinase assay system (Promega). In *mRad9*$^{+/+}$ mES cells, DNA-PKcs kinase activity increased significantly after etoposide treatment; in *mRad9*$^{-/-}$ mES cells, the increase of ^{32}P incorporation was marginal and statistically insignificant; in *mRad9*$^{-/-}$+*mRad9* mES cells, the incorporation of ^{32}P increased significantly after etoposide treatment, similar to that of *mRad9*$^{+/+}$ mES cells(Figure 5c). Our results indicate that Rad9 is critical for the activation of DNA-PKcs after DNA damage.

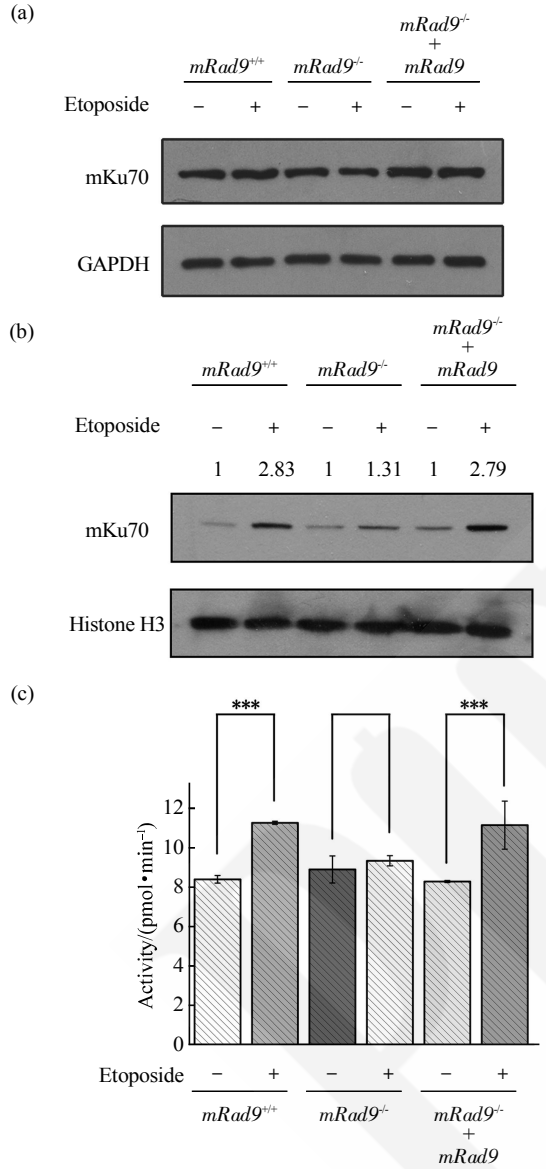

Fig. 5　Loss of Rad9 impairs Ku70 binding to chromatin and causes attenuated DNA-PKcs kinase activity

(a) Western blot analysis was performed. Cell lysates from *mRad9*$^{+/+}$ mES cells, *mRad9*$^{-/-}$ mES cells and *mRad9*$^{-/-}$+*mRad9* mES cells with or without etoposide treatment (30 min) were sequentially immunoblotted with antibody against mKu70 (top, 70 ku) and GAPDH (bottom, 36 ku). Neither loss of Rad9 nor DNA damage induced any obvious change of Ku70 at the protein level. (b) Chromatin binding assay was performed. Chromatin-bound proteins extracted from *mRad9*$^{+/+}$ mES cells, *mRad9*$^{-/-}$ mES cells and *mRad9*$^{-/-}$+*mRad9* mES cells with or without etoposide treatment (30 min) were sequentially immunoblotted with antibody against mKu70 (top, 70 ku) and Histone H3 (bottom, 17 ku). Numbers reflect the intensity of bands representing chromatin-bound mKu70 protein levels normalized to Histone H3 and compared to the sample without etoposide treatment. Ku70 recruitment was impaired in cells depleted of Rad9 after etoposide treatment. (c) DNA-PK kinase activity assay was performed. DNA-PK kinase activity was measured with the SignaTECT™ DNA-Dependent Protein kinase assay system (Promega). The amount of ^{32}P incorporated into the DNA-PK peptide substrate which was presented as mean±SD from three independent experiments indicated the DNA-PK kinase activity of the nuclear extract from *mRad9*$^{+/+}$ mES cells, *mRad9*$^{-/-}$ mES cells and *mRad9*$^{-/-}$+*mRad9* mES cells with or without etoposide treatment (30 min, *t*-test, ***P <0.01).

3　Discussion

In this study, we reported for the first time that Rad9 interacted with Ku70 physically (Figure 1–3) and functionally. Knockdown of Rad9 in human cells or *Rad9* deletion in mouse cells impaired NHEJ(Figure 4). *Rad9* deletion impairs Ku70 binding to chromatin and attenuated DNA-PKcs kinase activity after DNA damage (Figure 5). These data suggest that Rad9 plays a significant role in NHEJ *via* interacting with Ku70.

Pandita *et al*[40] reported that mammalian Rad9 interacted with Rad51, and inactivation of mammalian Rad9 also resulted in decreased HR repair for DSB. However, whether Rad9 participates in NHEJ remains controversial. Pandita *et al* used hRad9-immunodepleted extracts or extracts from Rad9 siRNA-treated HEK 293T cells to assay DNA end-joining activity. They reported that no difference in this activity was found in extracts with or without hRad9[40]. Canfield *et al*[52] reported that Rad9 was not needed for the repair/supercoiling of the plasmids with cohesive ends (plasmid cut with *Eco*R Ⅰ) in MM3MG epithelial mouse cells. However, the repair of incompatible ends (plasmid cut with *Eco*R Ⅰ and *Eco*R Ⅴ in presence of [α-^{32}P]dATP) does rely on Rad9[52]. In this study, we found that Rad9 knockdown in HEK 293T human cells as well as in mouse ES cells genetically deleted in Rad9 leads to a three to four-fold reduction in the DNA end-joining efficiency using the plasmid with cohesive ends (plasmid cut with *Eco*R Ⅰ). We further performed the antibody inhibition experiment in the extracts from HEK 293T cells. The *in vitro* end-joining assay is a well-characterized method. We performed the experiments according to Iliakis's report[43]. The discrepancies between our and Pandita's as well as Canfield's results are not well understood at present. We noticed that both our and Canfield's laboratories used *Eco*R Ⅰ-cut plasmid Bluescript. However, they analyzed the repair of the plasmids as formation of high mobility forms (supercoiling) which were the results of religation and simultaneous assembly of nucleosomes on the template. In our study, we analyzed the repair of the plasmids as formation of dimer and other higher multitimers which were the results of the end-joining activities presented in the extract. Furthermore, the cell models we used were different. Canfield *et al* used MM3MG epithelial mouse cells, and we used HEK 293T human cells and mouse ES cells. Whether the differences in cell models

contributed to the different results is inconclusive at the present. Both Pandita's[40] and our research groups used HEK 293T human cells, but the results were different (Figure 4d and 4e). One difference between us was that they only measured DNA dimer, but we measured dimer and multimers. In contrast to these two research groups, we also used mouse ES cells in which Rad9 was genetically deleted, and obtained the same results as for those of Rad9 knockdown human HEK 293T cells. Obviously, more studies will be needed to resolve or reconcile these differences.

In eukaryotes, Ku70 and Ku80 can form a stable heterodimeric complex and play a key role in NHEJ[27-28, 31]. It can bind the broken DNA ends with high affinity, hold the ends together, regulate the exonuclease activities at the DNA ends and recruit other repair factors to the site of DNA damage[51]. After binding to DSB ends, the regulatory subunit Ku heterodimer can recruit the catalytic subunit DNA-PKcs and trigger its serine/threonine kinase activity[30]. In this study, we found that Rad9 and Ku70 interacted physically and the physical interaction of Rad9 and Ku70 can be detected both in human HeLa cells and in mES cells (Figure 1 and 2). Furthermore, the interaction was functional. Reduction or deletion of Rad9 impaired Ku70 binding to chromatin after DNA damage (Figure 5b). Currently, the generally accepted working model is that Rad9, in complex with Rad1 and Hus1, binds to chromatin early in response to the DNA damage and serves as a recruiting platform for the downstream proteins involved in cell cycle arrest, DNA repair and apoptosis[18, 53-54]. Our results indicate that Rad9 also participates in the recruitment of Ku70 to the DNA damage region. Furthermore, we found that Rad9 deletion attenuated DNA-PKcs kinase activity after DNA damage (Figure 5c). DNA-PKcs relies on Ku proteins to recruit it to the broken DNA ends which then activates its kinase activity. The effects of Rad9 on DNA-PKcs kinase activity might be through Ku70 because loss of Rad9 impairs the recruitment of Ku70 to the DNA damage region. Besides its indirect effects, whether Rad9 can directly regulate the kinase activity of DNA-PKcs deserves further investigation.

It is well known that Rad9, Rad1 and Hus1 can form a PCNA-like ring structure, the 9-1-1 complex[2, 55-57]. Using co-immunoprecipitation assay, we observed weak interaction between HA-hRad1/HA-hHus1 and Flag-hKu70. Furthermore, the results of GST-pull down assay indicate that unlike Rad9, Rad1 and Hus1 did not interact with Ku70 physically. As reported by Xu *et al*[3], the 9-1-1 complex is a highly asymmetrical structure and has an extremely uneven charge distribution. These structural differences may explain the binding specificity of these three components observed in this study. Such asymmetrical interactions with the 9-1-1 complex have also been reported in other factors such as MYH[10] and Fen1[3]. However, our results can not exclude the possibility that hRad9's function in NHEJ is not in the 9-1-1 complex form. Further work using Rad1-deletion and Hus1-deletion cells will help to give a clearer answer to this question.

4 Conclusions

In this study, we found that Rad9 interacted with Ku70 physically and functionally. Knockdown of Rad9 in human cells or *Rad9* deletion in mouse cells impaired NHEJ. Furthermore, *Rad9* deletion impaired the binding of Ku70 to chromatin and attenuated DNA-PKcs kinase activity after DNA damage. These data suggest a novel role of Rad9 in mediating the NHEJ process *via* modulating the molecular activities of the DNA-PKcs/Ku70/Ku80 complex.

References

[1] Huen M S, Chen J. Assembly of checkpoint and repair machineries at DNA damage sites. Trends in Biochemical Sciences, 2010, **35**(2): 101-108

[2] Griffith J D, Lindsey-Boltz L A, Sancar A. Structures of the human Rad17-replication factor C and checkpoint Rad 9-1-1 complexes visualized by glycerol spray/low voltage microscopy. Journal of Biological Chemistry, 2002, **277**(18): 15233-15236

[3] Xu M, Bai L, Gong Y, *et al*. Structure and functional implications of the human rad9-hus1-rad1 cell cycle checkpoint complex. Journal of Biological Chemistry, 2009, **284**(31): 20457-20461

[4] Sohn S Y, Cho Y. Crystal structure of the human rad9-hus1-rad1 clamp. Journal of Molecular Biology, 2009, **390**(3): 490-502

[5] Doré A S, Kilkenny M L, Rzechorzek N J, *et al*. Crystal structure of the rad9-rad1-hus1 DNA damage checkpoint complex- implications for clamp loading and regulation. Molecular Cell, 2009, **34** (6): 735-745

[6] Hopkins K M, Auerbach W, Wang X Y, *et al*. Deletion of mouse rad9 causes abnormal cellular responses to DNA damage, genomic instability, and embryonic lethality. Molecular and Cellular Biology, 2004, **24**(16): 7235-7248

[7] Zhang C, Zhang C X, He Y, *et al*. Phosphorylation sites on Tyr28 and the C-terminus of Rad9 are required for inhibition of premature chromosomal condensation across the entire S phase. Cellular Physiology and Biochemistry, 2008, **22**(1-4): 295-306

[8] Zou L, Cortez D, Elledge S J. Regulation of ATR substrate selection

by Rad17-dependent loading of Rad9 complexes onto chromatin. Genes & Development, 2002, **16**(2): 198−208

[9] Edward A N, David C. ATR signalling: more than meeting at the fork. Biochemical Journal, 2011, **436**(3): 527−536

[10] Shi G, Chang D, Cheng C, *et al*. Physical and functional interactions between MutY glycosylase homologue (MYH) and checkpoint proteins Rad9-Rad1-Hus1. Biochem J, 2006, **400**(1): 53−62

[11] Guan X, Bai H, Shi G, *et al*. The human checkpoint sensor Rad9-Rad1-Hus1 interacts with and stimulates NEIL1 glycosylase. Nucleic Acids Research, 2007, **35**(8): 2463−2472

[12] Guan X, Madabushi A, Chang D-Y, *et al*. The human checkpoint sensor Rad9-Rad1-Hus1 interacts with and stimulates DNA repair enzyme TDG glycosylase. Nucleic Acids Research, 2007, **35**(18): 6207−6218

[13] Gembka A, Toueille M, Smirnova E, *et al*. The checkpoint clamp, Rad9-Rad1-Hus1 complex, preferentially stimulates the activity of apurinic/apyrimidinic endonuclease 1 and DNA polymerase β in long patch base excision repair. Nucleic Acids Research, 2007, **35**(8): 2596−2608

[14] Friedrich-Heineken E, Toueille M, Tännler B, *et al*. The two DNA clamps Rad9/Rad1/Hus1 complex and proliferating cell nuclear antigen differentially regulate flap endonuclease 1 activity. Journal of Molecular Biology, 2005, **353**(5): 980−989

[15] Song W, Levin D S, Varkey J, *et al*. A conserved physical and functional interaction between the cell cycle checkpoint clamp loader and DNA ligase I of eukaryotes. Journal of Biological Chemistry, 2007, **282**(31): 22721−22730

[16] Wang W, Lindsey-Boltz L A, Sancar A, *et al*. Mechanism of stimulation of human DNA ligase I by the Rad9-Rad1-Hus1 checkpoint complex. Journal of Biological Chemistry, 2006, **281**(30): 20865−20872

[17] He W, Zhao Y, Zhang C, *et al*. Rad9 plays an important role in DNA mismatch repair through physical interaction with MLH1. Nucleic Acids Research, 2008, **36**(20): 6406−6417

[18] Bai H, Madabushi A, Guan X, *et al*. Interaction between human mismatch repair recognition proteins and checkpoint sensor Rad9-Rad1-Hus1. DNA Repair, 2010, **9**(5): 478−487

[19] Li T, Wang Z, Zhao Y, *et al*. Checkpoint protein Rad9 plays an important role in nucleotide excision repair. DNA Repair, 2013, **12**(4): 284−292

[20] Warmerdam D O, Freire R, Kanaar R, *et al*. Cell cycle-dependent processing of DNA lesions controls localization of Rad9 to sites of genotoxic stress. Cell Cycle, 2009, **8**(11): 1765−1774

[21] Burtelow M A, Kaufmann S H, Karnitz L M. Retention of the human Rad9 checkpoint complex in extraction-resistant nuclear complexes after DNA damage. Journal of Biological Chemistry, 2000, **275**(34): 26343−26348

[22] Greer D A, Besley B D A, Kennedy K B, *et al*. hRad9 rapidly binds DNA containing double-strand breaks and is required for damage-dependent topoisomerase Ⅱ beta binding protein 1 focus formation. Cancer Research, 2003, **63**(16): 4829−4835

[23] West S C. Molecular views of recombination proteins and their control. Nature Reviews Molecular Cell Biology, 2003, **4**(6): 435−445

[24] Lieber M R. The mechanism of double-strand DNA break repair by the nonhomologous DNA end joining pathway. Annual Review of Biochemistry, 2010, **79**(1): 181−211

[25] Chapman J R, Taylor M R, Boulton S J. Playing the end game: DNA double-strand break repair pathway choice. Molecular Cell, 2012, **47**(4): 497−510

[26] Summers K, Shen F, Sierra Potchanant E, *et al*. Phosphorylation: the molecular switch of double-strand break repair. International Journal of Proteomics, 2011, **2011**(1): 373816

[27] Mimori T, Hardin J A. Mechanism of interaction between Ku protein and DNA. Journal of Biological Chemistry, 1986, **261**(22): 10375−10379

[28] Blier P R, Griffith A J, Craft J, *et al*. Binding of Ku protein to DNA. Measurement of affinity for ends and demonstration of binding to nicks. Journal of Biological Chemistry, 1993, **268**(10): 7594−7601

[29] Walker J R, Corpina R A, Goldberg J. Structure of the Ku heterodimer bound to DNA and its implications for double-strand break repair. Nature, 2001, **412**(6847): 607−614

[30] Rivera-Calzada A, Spagnolo L, Pearl L H, *et al*. Structural model of full-length human Ku70-Ku80 heterodimer and its recognition of DNA and DNA-PKcs. EMBO Reports, 2007, **8**(1): 56−62

[31] Meek K, Gupta S, Ramsden D A, *et al*. The DNA-dependent protein kinase: the director at the end. Immunological Reviews, 2004, **200**(1): 132−141

[32] Jovanovic M, Dynan W S. Terminal DNA structure and ATP influence binding parameters of the DNA-dependent protein kinase at an early step prior to DNA synapsis. Nucleic Acids Research, 2006, **34**(4): 1112−1120

[33] Cui X, Yu Y, Gupta S, *et al*. Autophosphorylation of DNA-dependent protein kinase regulates DNA end processing and may also alter double-strand break repair pathway choice. Molecular and Cellular Biology, 2005, **25**(24): 10842−10852

[34] Lieberman H B, Hopkins K M, Nass M, *et al*. A human homolog of the *Schizosaccharomyces pombe* rad9+ checkpoint control gene. Proc Natl Acad Sci USA, 1996, **93**(24): 13890−13895

[35] Murray J M, Carr A M, Lehmann A R, *et al*. Cloning and characterisation of the rad9 DNA repair gene from *Schizosaccharomyces pombe*. Nucleic Acids Research, 1991, **19**(13): 3525−3531

[36] Sunnerhagen P, Seaton B, Nasim A, *et al*. Cloning and analysis of a gene involved in DNA repair and recombination, the rad1 gene of *Schizosaccharomyces pombe*. Molecular and Cellular Biology, 1990, **10**(7): 3750−3760

[37] Han L, Hu Z, Liu Y, *et al*. Research mouse Rad1 deletion enhances susceptibility for skin tumor development. Molecular Cancer, 2010, **9**(1): 67−79

[38] Zhang C, Liu Y, Hu Z, *et al*. Targeted deletion of mouse Rad1 leads to deficient cellular DNA damage responses. Protein & Cell, 2011, **2**(5): 410−422

[39] Wang X, Hu B, Weiss R, *et al*. The effect of Hus1 on ionizing radiation sensitivity is associated with homologous recombination repair but is independent of nonhomologous end-joining. Oncogene, 2006, **25**(13): 1980-1983

[40] Pandita R K, Sharma G G, Laszlo A, *et al*. Mammalian Rad9 plays a role in telomere stability, S-and G2-phase-specific cell survival, and homologous recombinational repair. Molecular and Cellular Biology, 2006, **26**(5): 1850-1864

[41] Tsai F-L, Kai M. The checkpoint clamp protein Rad9 facilitates DNA-end resection and prevents alternative non-homologous end joining. Cell Cycle, 2014, **13**(21): 3460-3464

[42] Hang H, Lieberman H B. Physical interactions among human checkpoint control proteins HUS1p, RAD1p, and RAD9p, and implications for the regulation of cell cycle progression. Genomics, 2000, **65**(1): 24-33

[43] Iliakis G, Rosidi B, Wang M, *et al*. Plasmid-based assays for DNA end-joining *in vitro* [M]. DNA Repair Protocols: Mammalian Systems. Humana Press. 2006: 123-131

[44] Mé ndez J, Stillman B. Chromatin association of human origin recognition complex, cdc6, and minichromosome maintenance proteins during the cell cycle: assembly of prereplication complexes in late mitosis. Molecular and Cellular Biology, 2000, **20** (22): 8602-8612

[45] Onge R P S, Udell C M, Casselman R, *et al*. The human G2 checkpoint control protein hRAD9 is a nuclear phosphoprotein that forms complexes with hRAD1 and hHUS1. Molecular Biology of the Cell, 1999, **10**(6): 1985-1995

[46] Kinner A, Wu W Q, Staudt C, *et al*. gamma-H2AX in recognition and signaling of DNA double-strand breaks in the context of chromatin. Nucleic Acids Research, 2008, **36**(17): 5678-5694

[47] Hu Z, Liu Y, Zhang C, *et al*. Targeted deletion of Rad9 in mouse skin keratinocytes enhances genotoxin-induced tumor development. Cancer Research, 2008, **68**(14): 5552-5561

[48] An L, Wang Y, Liu Y, *et al*. Rad9 is required for B cell proliferation and immunoglobulin class switch recombination. Journal of Biological Chemistry, 2010, **285**(46): 35267-35273

[49] Mladenov E, Iliakis G. Induction and repair of DNA double strand breaks: the increasing spectrum of non-homologous end joining pathways. Mutation Research/Fundamental and Molecular Mechanisms of Mutagenesis, 2011, **711**(1): 61-72

[50] Gu B-W, Bessler M, Mason P J. A pathogenic dyskerin mutation impairs proliferation and activates a DNA damage response independent of telomere length in mice. Proc Natl Acad Sci USA, 2008, **105**(29): 10173-10178

[51] Downs J A, Jackson S P. A means to a DNA end: the many roles of Ku. Nature Reviews Molecular Cell Biology, 2004, **5**(5): 367-378.

[52] Canfield C, Rains J, De Benedetti A. TLK1B promotes repair of DSBs *via* its interaction with Rad9 and Asf1. BMC Molecular Biology, 2009, **10**(1): 110

[53] Delacroix S, Wagner J M, Kobayashi M, *et al*. The Rad9-Hus1-Rad1 (9-1-1) clamp activates checkpoint signaling *via* TopBP1. Genes & Development, 2007, **21**(12): 1472-1477

[54] Komatsu K, Miyashita T, Hang H, *et al*. Human homologue of S. pombe Rad9 interacts with BCL-2/BCL-x L and promotes apoptosis. Nature Cell Biology, 2000, **2**(1): 1-6

[55] Lindsey-Boltz L A, Bermudez V P, Hurwitz J, *et al*. Purification and characterization of human DNA damage checkpoint Rad complexes. Proc Natl Acad Sci USA, 2001, **98**(20): 11236-11241

[56] Shiomi Y, Shinozaki A, Nakada D, *et al*. Clamp and clamp loader structures of the human checkpoint protein complexes, Rad9-1-1 and Rad17-RFC. Genes to Cells, 2002, **7**(8): 861-868

[57] Venclovas C, Thelen M P. Structure-based predictions of Rad1, Rad9, Hus1 and Rad17 participation in sliding clamp and clamp-loading complexes. Nucleic Acids Research, 2000, **28**(13): 2481-2493

细胞周期监控点蛋白 Rad9 与非同源末端连接修复蛋白 Ku70 的相互作用研究 *

范英俊[1,2)**]　刘宇恒[1,2)**]　王玉兰[1,2)**]　孔冰洁[1,2)]　赵　云[1)]
叶　琛[1)]　安莉莉[1)***]　杭海英[1)***]

([1)] 中国科学院生物物理研究所生物大分子国家重点实验室，蛋白质与多肽药物所重点实验室，北京 100101；
[2)] 中国科学院大学，北京 100049)

摘要　Rad9 是一种重要的细胞周期监控点调控蛋白．越来越多的证据显示，Rad9 也可与多种 DNA 损伤修复通路中的蛋白质相互作用，并调节其功能，在 DNA 损伤修复中发挥重要作用．非同源末端连接修复是 DNA 双链断裂的一条重要修复途径．Ku70、Ku80 和 DNA 依赖的蛋白激酶催化亚基(DNA-PKcs)共同组成 DNA 依赖的蛋白激酶复合物(DNA-PK)，在非同源末端修复连接中起重要作用．本研究中，检测到 Rad9 与 Ku70 有直接的物理相互作用和功能相互作用．我们在不同的细胞模型中发现，Rad9 基因敲除、Rad9 蛋白去除或 Rad9 表达降低会导致非同源末端连接效率明显下降．已有的研究表明，DNA 损伤可导致细胞中 Ku70 与染色质结合增加及 DNA-PKcs 激酶活性增强．我们的结果显示，与野生小鼠细胞相比，Rad9 基因敲除的小鼠细胞中， DNA 损伤诱导的上述效应均减弱．综上所述，我们的研究首次报道了 Rad9 与非同源末端连接修复蛋白 Ku70 间有相互作用，并提示 Rad9 可通过调节 Ku70/Ku80/DNA-PKcs 复合物功能参与非同源末端连接修复．

关键词　Rad9，非同源末端连接修复，Ku70，DNA 依赖的蛋白激酶催化亚基
学科分类号　Q2，Q7　　**DOI**: 10.16476/j.pibb.2018.0163

* 国家自然科学基金资助项目(31370792, U1738112).
** 并列第一作者.
*** 通讯联系人.
安莉莉. Tel: 010-64888268, E-mail: afxdxz@163.com
杭海英. Tel: 010-64888473, E-mail: hh91@ibp.ac.cn
收稿日期：2018-06-11，接受日期：2018-08-29